



Computational Screening of Inhibitors for Malaria Treatment Against *Plasmodium Falciparum* Phosphatidylinositol 4-Kinase

Nomagugu B. Ncube¹, Matshawandile Tukulula^{1*}, Krishna K. Govender^{2*}

¹School of Chemistry and Physics, College of Agriculture, Engineering and Science (CAES) University of KwaZulu-Natal, Westville Campus, Durban 4001, South Africa

²Department of Chemical Sciences University of Johannesburg, Doornfontein Campus P.O. Box 17011, Johannesburg 2028, South Africa, National Institute for Theoretical and Computational Sciences, NITheCS Stellenbosch 7602, South Africa.

Corresponding author: Krishna K. Govender, Department of Chemical Sciences University of Johannesburg, Doornfontein Campus P.O. Box 17011, Johannesburg 2028, South Africa, National Institute for Theoretical and Computational Sciences, NITheCS Stellenbosch 7602, South Africa. Tel: + 27 11 559 6180; E-mail: krishnag@uj.ac.za.

Received: January 25, 2025; **Accepted:** March 23, 2025; **Published:** March 31, 2025

© **Copyright 2025:** Govender et al. This is an open access article distributed under the terms of the Creative Commons Attribution License [CC-BY 4.0.], which permits unrestricted use, distribution, and reproduction in any medium, provided the original author and source are credited.

Abstract

In this study, we present a follow-up on a homology model that was developed and characterised previously in our group. A structure-based virtual screening approach to screen various chemical libraries in a quest to find new or novel inhibitors for the *Plasmodium falciparum* phosphatidylinositol 4-kinase type III beta (*PfPI4KIIIβ*) enzyme was the main focus. Virtual screening of the various Maybridge, Medicines for Malaria Venture (MMV) and Pubmed libraries, using Schrödinger Suites, revealed several potential hit compounds. Of the 229 944 compounds screened, 175 hits were found after the extra precision (XP) docking cascade. The top three hits, namely **007**, **009** and **018**, based on the XP docking scores > -8.5 kcal/mol were subjected to molecular dynamics (MD) simulations. Hit compound **018**, from the Maybridge_GPCR library, had the best root mean square deviation (RMSD) and molecular mechanics with generalised Born and surface area solvation (MM/GBSA) results compared to the known ligand, MMV048, for this enzyme. Interestingly, **018** interacted with polar serine and hydrophobic leucine, whereas MMV048 primarily interacted with the hydrophobic valine in the active site of *PfPI4KIIIβ*. Furthermore, **018** exhibited more hydrogen bond interactions than the known ligand. The ligand-torsion plot undertaken on **018** and MMV048 indicated that **018** is more rigid than MMV048 and this implies better binding to the active site. The MM/GBSA studies indicated MMV048 has a lower solvation score of 1.2528, hence its inferior binding interactions compared to **018** (solvation score of 25.1432). Thus, virtual screening of known libraries can potentially provide new hit compounds and is a good starting point for structure-activity relation (SAR) studies while saving time, costs and resources.

Keywords: Virtual screening (VS); MM/GBSA; VSGB; OPLS4; PfPI4KIIIβ

Introduction

Malaria is a tropical disease that is transmitted by the Anopheles female mosquito.[1] Malaria's presence is rampaging the subtropical regions and sub-Saharan Africa, regions that provide an optimum environment for the mosquito vectors to breed. Most of the malaria-causing plasmodium species have double lifecycles, one in the vector and the other in the human host.[2] The present challenge is treatment failures due to the development of drug-resistant mutants of the malaria-causing parasite. Drug resistance results from plasmodium species mutating to avoid attenuation of currently used medication. Spontaneous chromosomal point mutations or gene duplications create resistant mutants with survival advantage in the presence of the antimalarial drugs. Another cause of drug resistance may be due to patients not adhering to treatment regimes or patients exposed to sub-optimal therapeutic concentrations of the currently used drugs.[3–5]

Malaria has been managed to a certain degree by non-pharmacological interventions, including mosquito nets[6], getting rid of stagnant water[7], and fumigating.[8] However, it remains uncontrollable due to the constant emergence of resistant strains.[9] Therefore, there is an ongoing search in the research community for new inhibitors that can target parasite development in either the host, vector, or both stages. Recent research has zoomed in on an enzyme that has shown significant importance in parasite development in both the vector and host. The enzyme in question, *Plasmodium falciparum* phosphatidylinositol 4-kinase type III beta (*PI4KIIIβ*), is a ubiquitous eukaryotic enzyme involved in lipids' phosphorylation and it plays a vital role in the regulation of intracellular signal transduction mechanisms.[4] It has been validated as the first known drug target that is required across all *Plasmodium* lifecycle stages.[10,11] There is currently no crystal structure for this enzyme[12,13], which limits its utility in virtual drug discovery studies; hence, developing a homology model and characterizing it is critical.

Previously, we had reported on the homology model that was generated from the 3D coordinates of the human kinase, PI4K (PDB 4D0L), template and the binding pocket characterization of the developed model, where key amino acid residues that interact with known inhibitors of this enzyme were identified.[14] The critical amino acid residues, Lys 549, and Val 598 in PI4K were conserved in *PfPI4KIIIβ* as Lys 347 and Val 396. In the current study, we wish to use the previously reported model to undertake the virtual high-throughput screening of various database libraries, displayed in **Table 1**, in our quest to find new inhibitors of *PfPI4KIIIβ*. In total, 14 libraries that consisted of 229 944 compounds were virtually screened as a single curated file. The most active compounds, ranked as the top three (3) compounds, were identified as potential new inhibitors. A structure-based approach was followed to find new inhibitors for *PfPI4KIIIβ*. This approach entails using the 3D structures of biological targets such as enzymes to identify potential bioactive chemical structures, termed inhibitors in our case. [15]

Table 1: Libraries screened during VS.

Library	Number of compounds
Maybridge_Building_Blocks_USD*	5124
Maybridge_GPCR_Library*	14053

Maybridge_HDAC_Library*	4107
Maybridge_HitCreator_V2*	14000
Maybridge_HitDiscover*	51775
Maybridge_IonChannel_Library*	6122
Maybridge_Kinase_Library*	10674
Maybridge_PPI_Library*	8349
Maybridge_Screening_Collection*	53399
Maybridge_Screening_Fragments*	58698
MMV-Global Health Priority Box [#]	480
MMV-Pandemic Response Box ^{&}	400
MMV-Analogs [§] (481
Miscilenous small collection	2282
Total	229944

*MaybridgeTlibraries were downloaded from the Thermo Fisher Scientific website (<https://www.thermofisher.com/za/en/home/industrial/pharma-biopharma/drug-discovery-development/screening-compounds-libraries-hit-identification.html> 12/09/2023); [#]MMV Global Health Priority Box compound structures were downloaded from the Medicines for Malaria Venture website (<https://www.mmv.org/mmv-open/global-health-priority-box/about-global-health-priority-box>; 12/09/2023); [&]MMV Pandemic Response Box compound structures (<https://www.mmv.org/mmv-open/pandemic-response-box/about-pandemic-response-box>; 12/09/2023); [§]MMV analogs (<https://www.mmv.org/mmv-open/malaria-libre/malaria-libre-data-repository>)

Results and Discussion

Homology model

The homology model shown in **Figure 1** was previously characterized and described by Ncube *et al.* (2023)[14] and was used in this study.

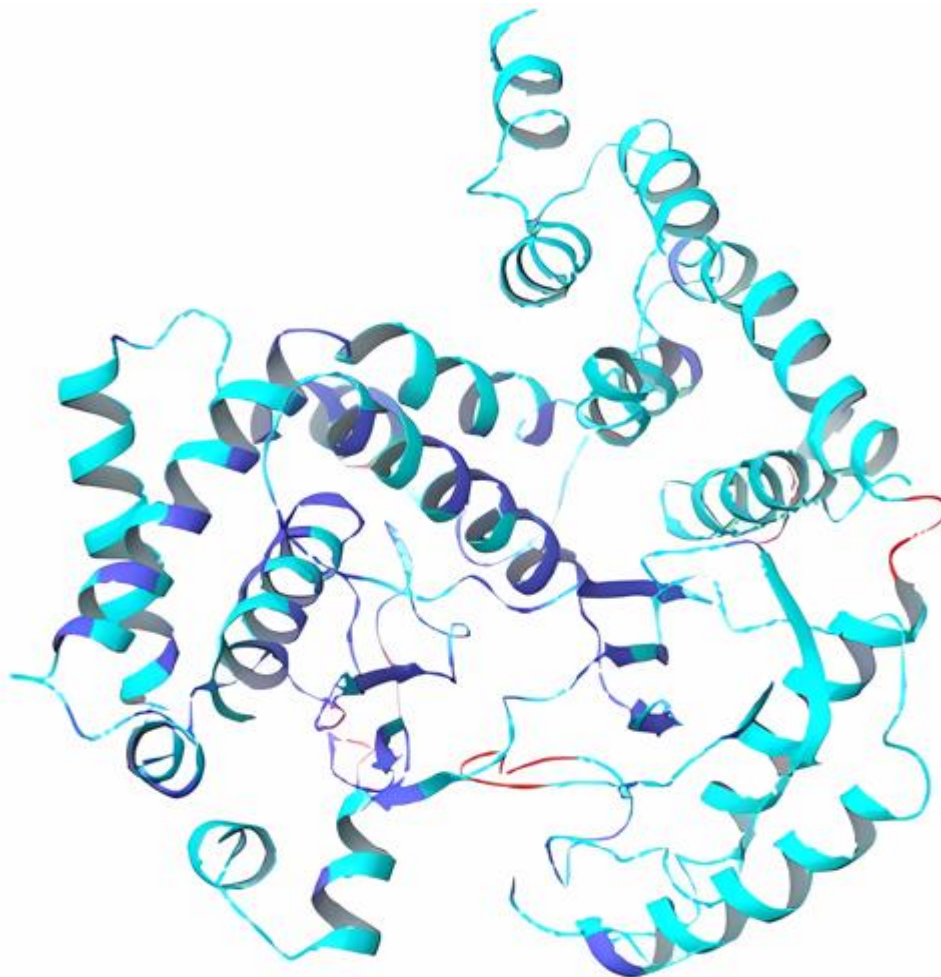


Figure 1: Homology model of *PfPI4K* previously described by Ncube *et al.* [9]

Virtual Screening (VS)

VS follows a three-step cycle:

- 1) High-Throughput Virtual Screening (HTVS) - elimination of ligands whose volume exceeds the binding site volume;
- 2) Standard Precision (SP); and
- 3) Extra Precision (XP) - slow and intensive algorithms that predict the binding chemistry of the ligands.

Both XP and SP docking use the same scoring function: SP, however, reduces the number of intermediate conformations as they travel down the docking funnel.[16] In addition, it reduces the thoroughness of the final torsional refinement and sampling. The docking algorithm remains the same in both XP and SP. XP, on the other hand, does more extensive sampling than SP.[17] It employs a more sophisticated scoring function with stringent requirements for ligand-receptor shape complementarity. This is a crucial step as it weeds out false positives that went through SP. XP provided a total of 175 hits presented in supplementary **Table S1**.

Molecular dynamics (MD) simulations of top hits

Compounds that showed docking scores > -8.5 kcal/mol were then selected for MD, and only three (3) compounds met this criterion. These top 3 hits (Set A in **Figure 2**) were subjected to MD simulation for optimization. Ligand **007** and **018** are from the Maybridge_GPCR_Library, whereas ligand **009** is from the Maybridge_Kinase_Library. They were then compared to the two experimentally validated ligands, **MMV048** and **5S8** (Set B in **Figure 3**), for *PfPI4KIII β* to ascertain if they possessed better binding properties as this would be the most desirable result. These two known ligands were previously used to characterize the binding pocket in our previous study. [9]

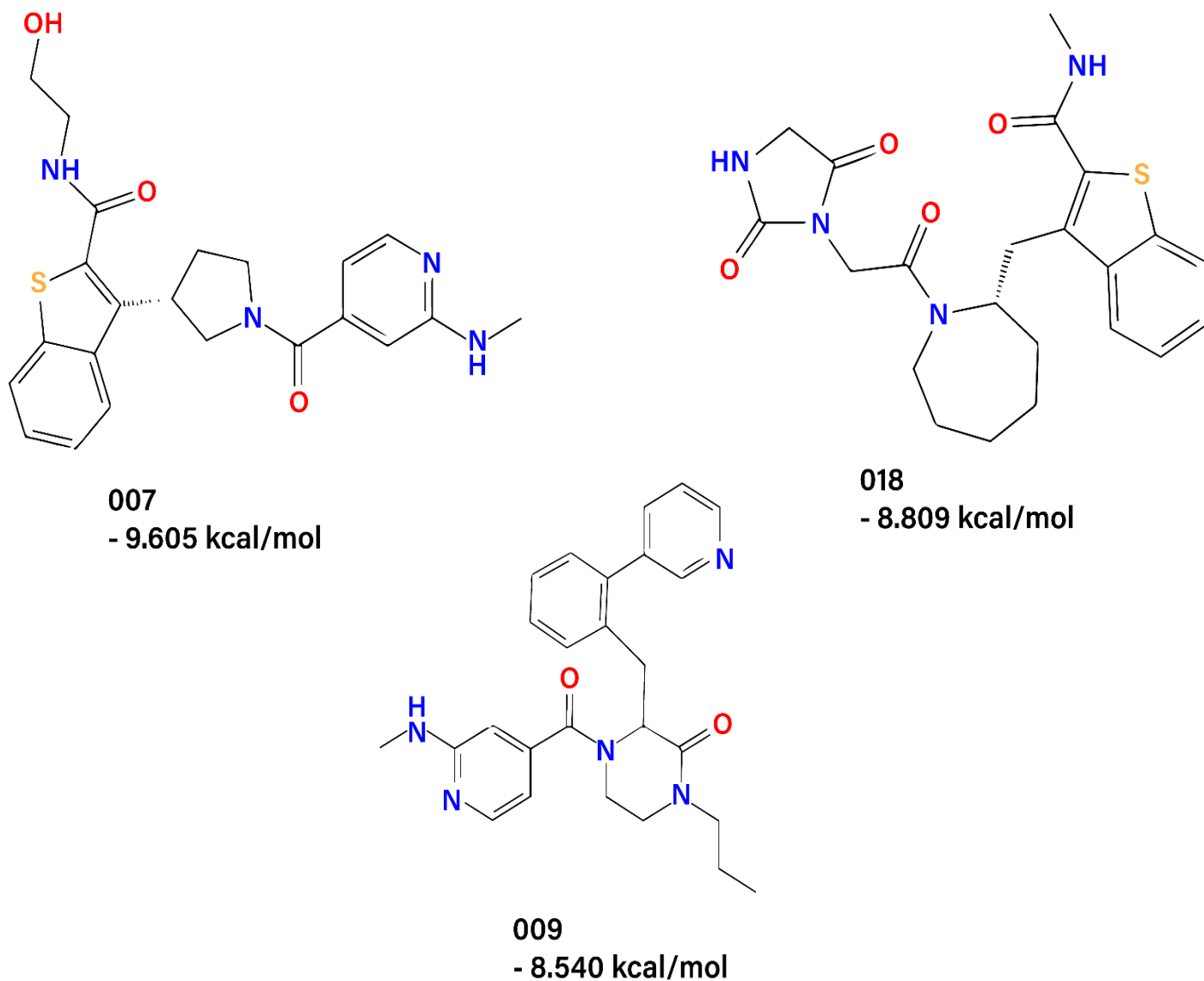


Figure 2: Set A (hits from VS) with their docking scores.

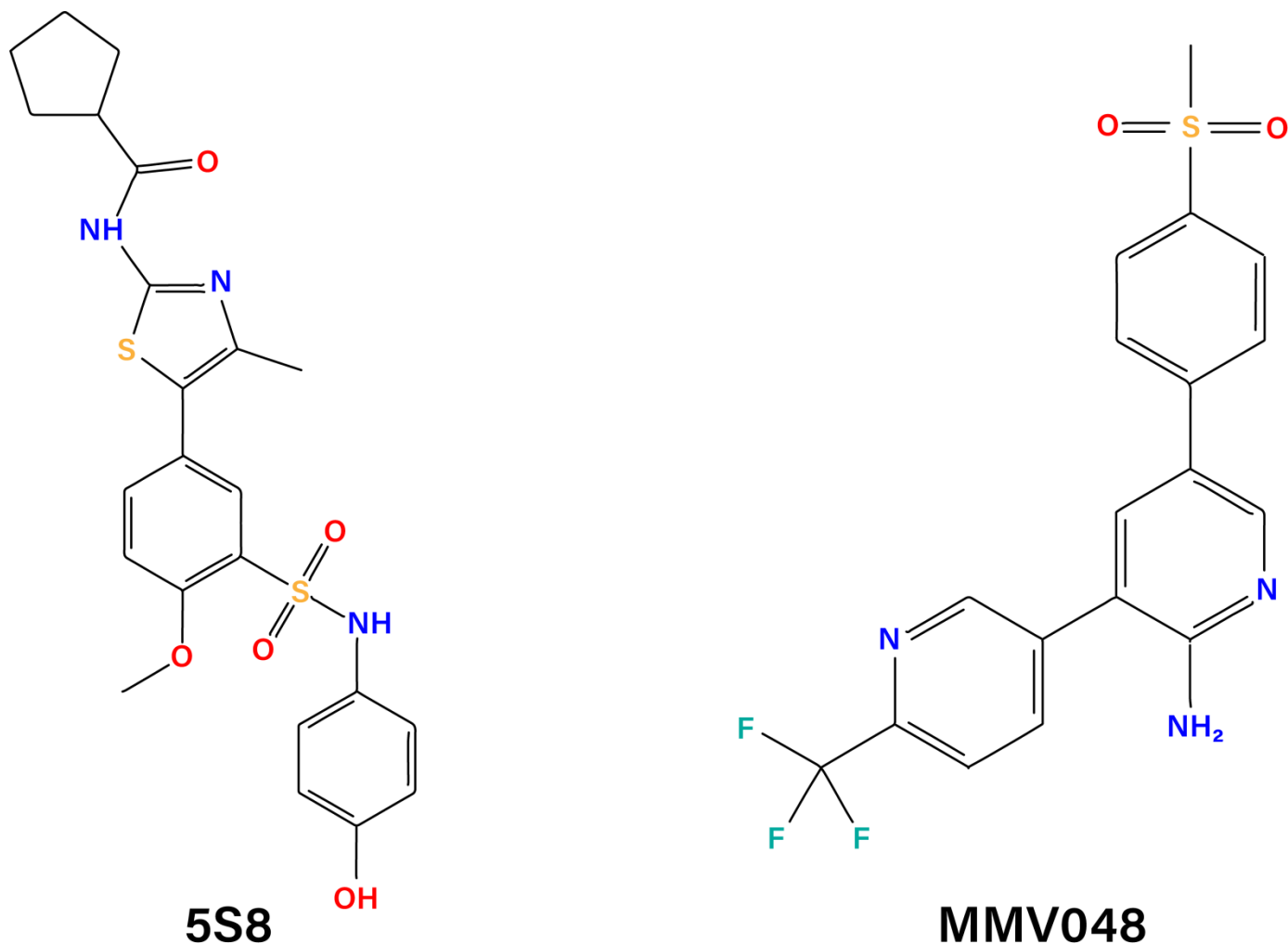


Figure 3: Set B (ligands with confirmed inhibitory activity).

The figures below are the RMSD graphs of the hit ligands in set A: **Figure 4** (for **018**), **Figure 5** (for **009**) and **Figure 6** (for **007**). The RMSD graphs for ligands **007** and **009** did not converge, meaning the simulation did not reach a state of equilibrium or stability. This may be due to the ligands not interacting properly with the binding pocket; in other words, they are not a perfect fit. Although the protein RMSD was high for ligand **018**, the system stabilized efficiently, and ligand stability is observed from approximately 75 ns of the simulation.

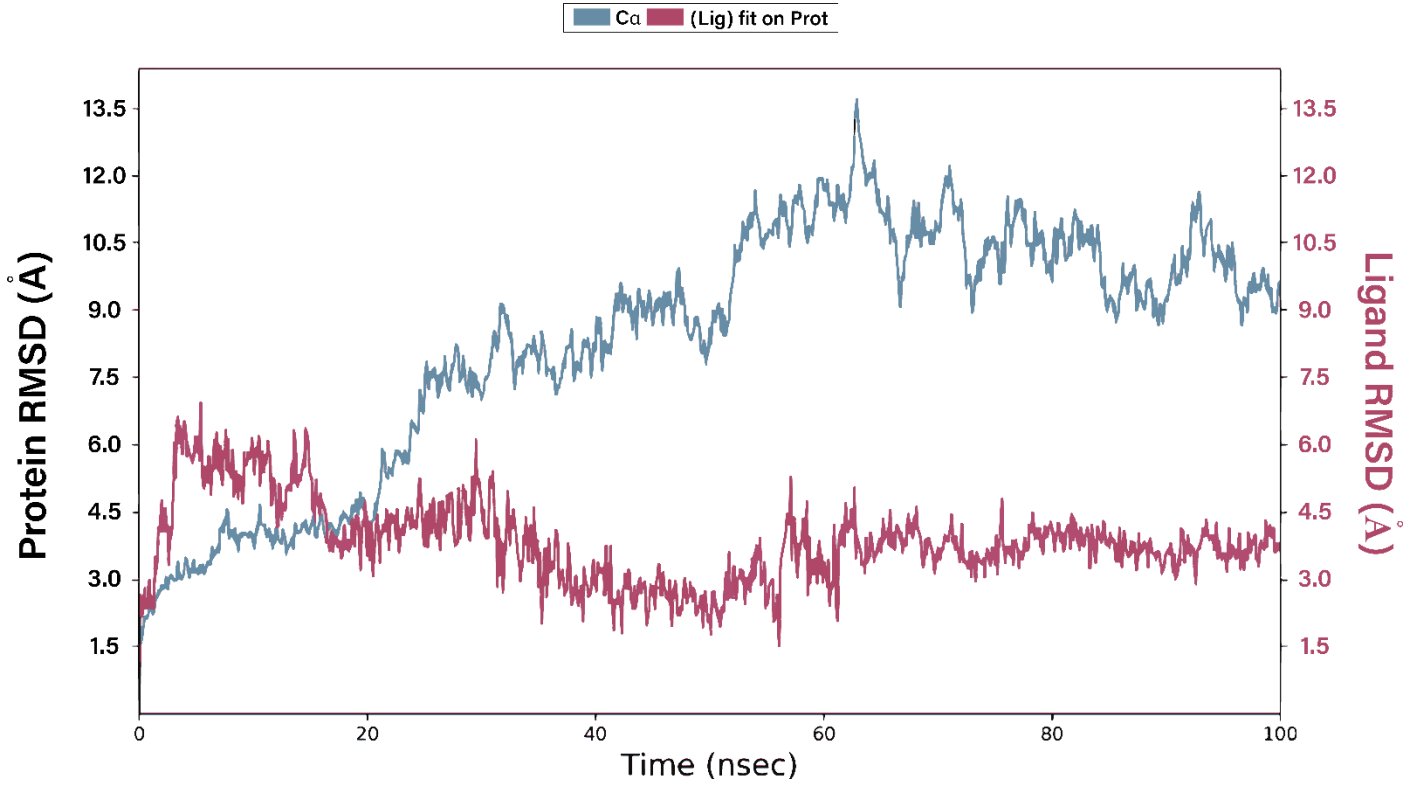


Figure 4: RMSD of ligand 018.

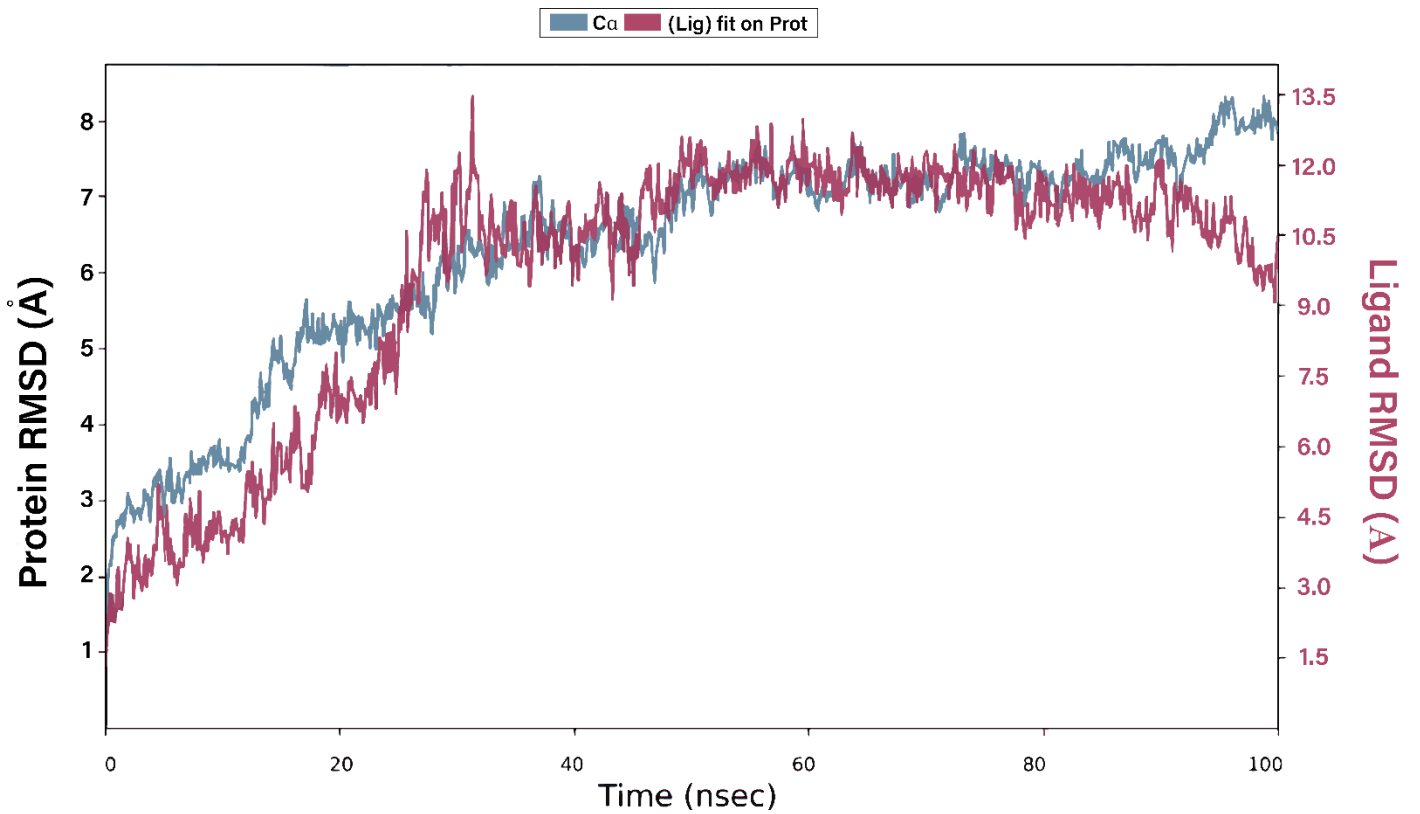
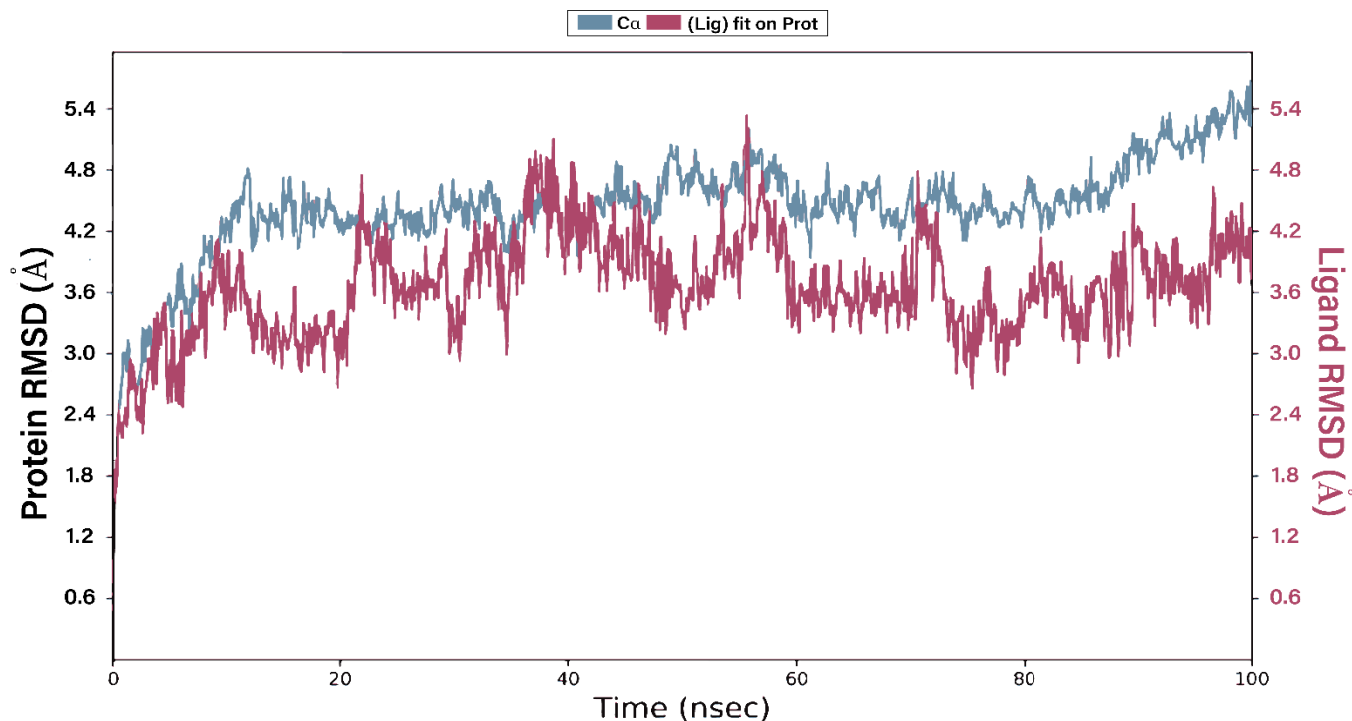


Figure 5: RMSD of ligand **009**.**Figure 6:** RMSD of ligand **007**.

A high RMSD value may be due to the initial positions of ligands and proteins in the docked complex or system complexity.[18] The key is to observe system stability and equilibration. Further computational processes, such as molecular mechanics with generalized Born and surface area solvation (MM/GBSA) also assist in establishing ligand-protein stability, as RMSD alone cannot be the determining factor.[19] The ligand RMSD (red) is way lower than the protein RMSD (blue) in **Figure 4**, meaning it does not exit the binding pocket. Physical visualization of the MD movie confirmed that the ligand did not exit the binding pocket. Based on these RMSD results, ligand **018** was selected as the best hit.

Ligand-protein contact

The following diagrams, **Figures 7** and **8**, show the ligand-protein contacts during MD. They displays interactions that the ligand (**018**) and MMV048 had with the protein for more than 30% of the simulation time. The results indicate that **018** mainly interacted with polar serine and hydrophobic leucine, whereas MMV048 primarily interacted with the hydrophobic valine. This may suggest that the hit ligand attracts more amino acids than the used known inhibitor of *PfPI4K*.

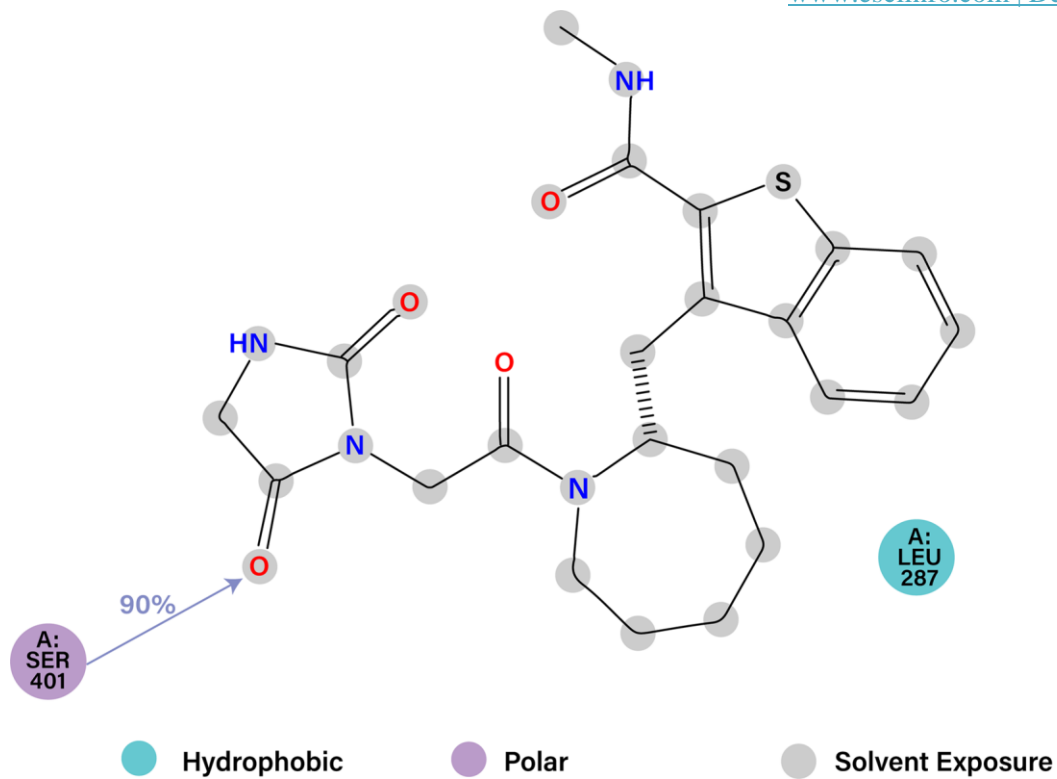


Figure 7: Ligand-protein contact of **018**.

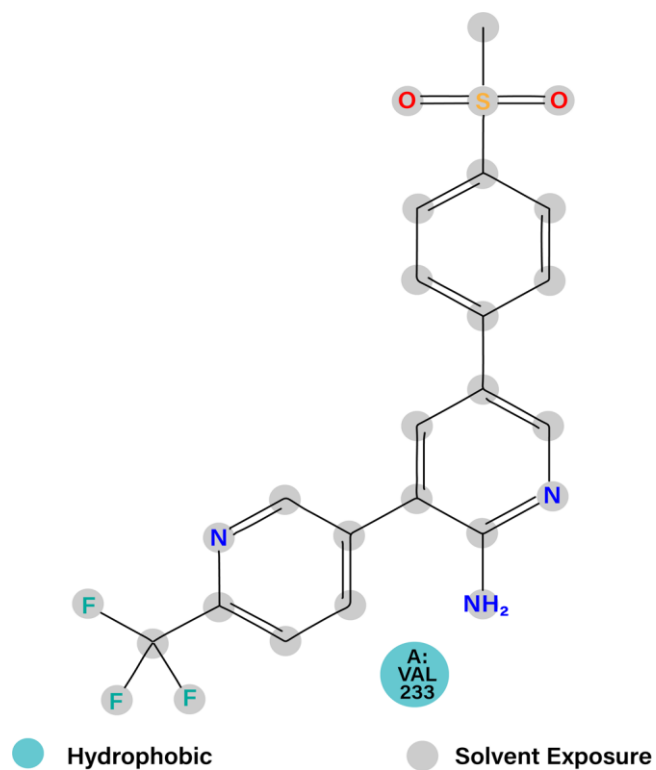


Figure 8: Ligand-protein contact of **MMV048**.

Figure 9 is an expansion of **Figures 7** and **8**. It categorizes the ligand-protein interactions or simply puts the ‘contacts’ into four types: hydrogen bonds, hydrophobic interactions, ionic interactions and water bridges. These interactions are monitored throughout the simulation and show when specific interactions were maintained. For example, a value of 0.6 means that the interaction between the ligand and the specific amino acid took place 60% of the simulation time. We can observe from **Figure 9** that ligand **018** had more hydrogen bonding than MMV048 (shown in **Figure 10**). Hydrogen bonds are the strongest intermolecular forces and are vital for forming the ligand-substrate complex.[20] MMV048 mostly interacted with hydrophobic residues. None of the ligands interacted with ionic residues.

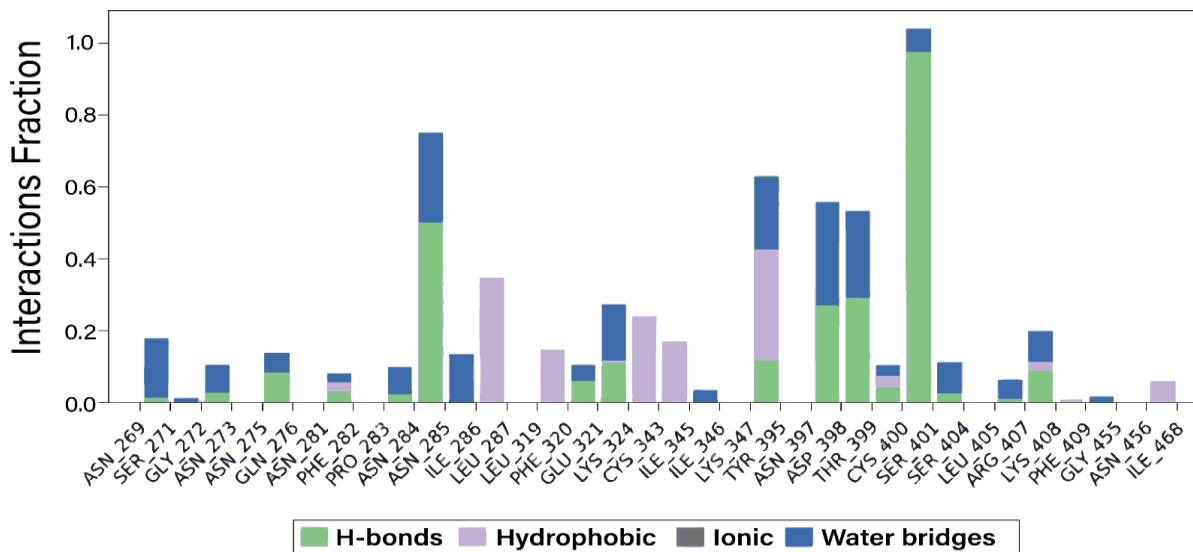


Figure 9: Protein-ligand contact diagram of **018**.

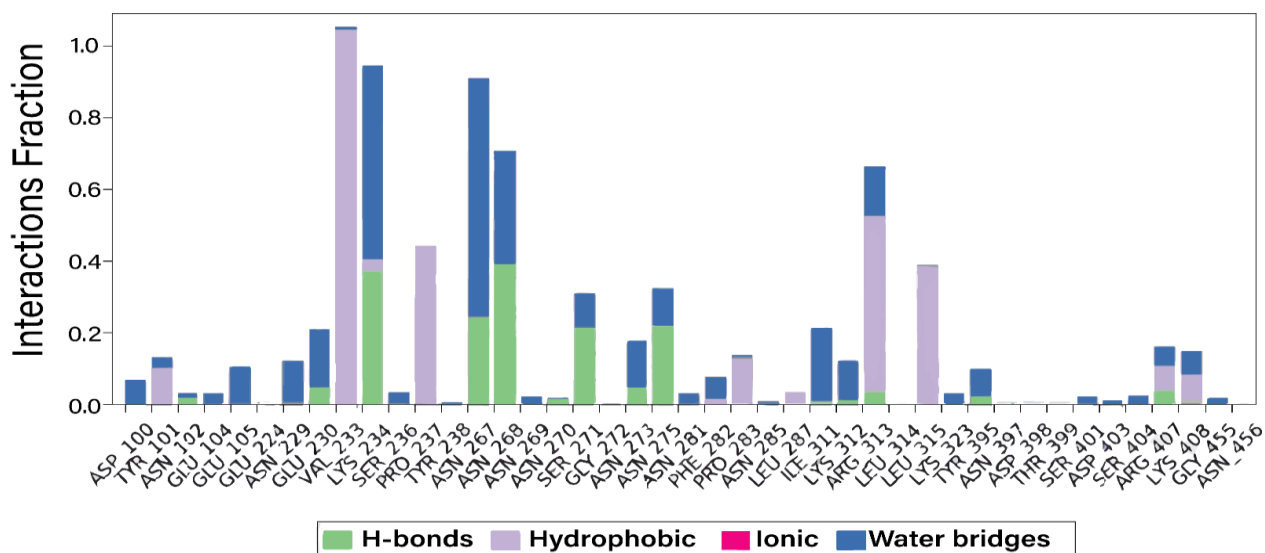


Figure 10: Protein-Ligand Contact diagram of **MMV048**.

Ligand torsion plot

Figures 11 and 12 are ligand torsion plots that summarize the conformation of every rotatable bond in the ligand during the simulation trajectory. The top panel of the figure, part a, is a 2D configuration of the ligand with color-coded rotatable bonds. Each rotatable bond is then accompanied by dial plots and bar plots of the same colour. The dial plots, also known as radial plots, represent the torsion conformation throughout the simulation. The simulation commences in the center of the radial plot, and the time elapsed is plotted radially outwards. The bar plots summarize the data on the radial plots in the form of a probability density of the torsion. Ligands with more rotatable bonds have increased conformational heterogeneity, meaning they bind better to the active site, whereas ligands with less rotatable bonds tend to be more rigid.[21]

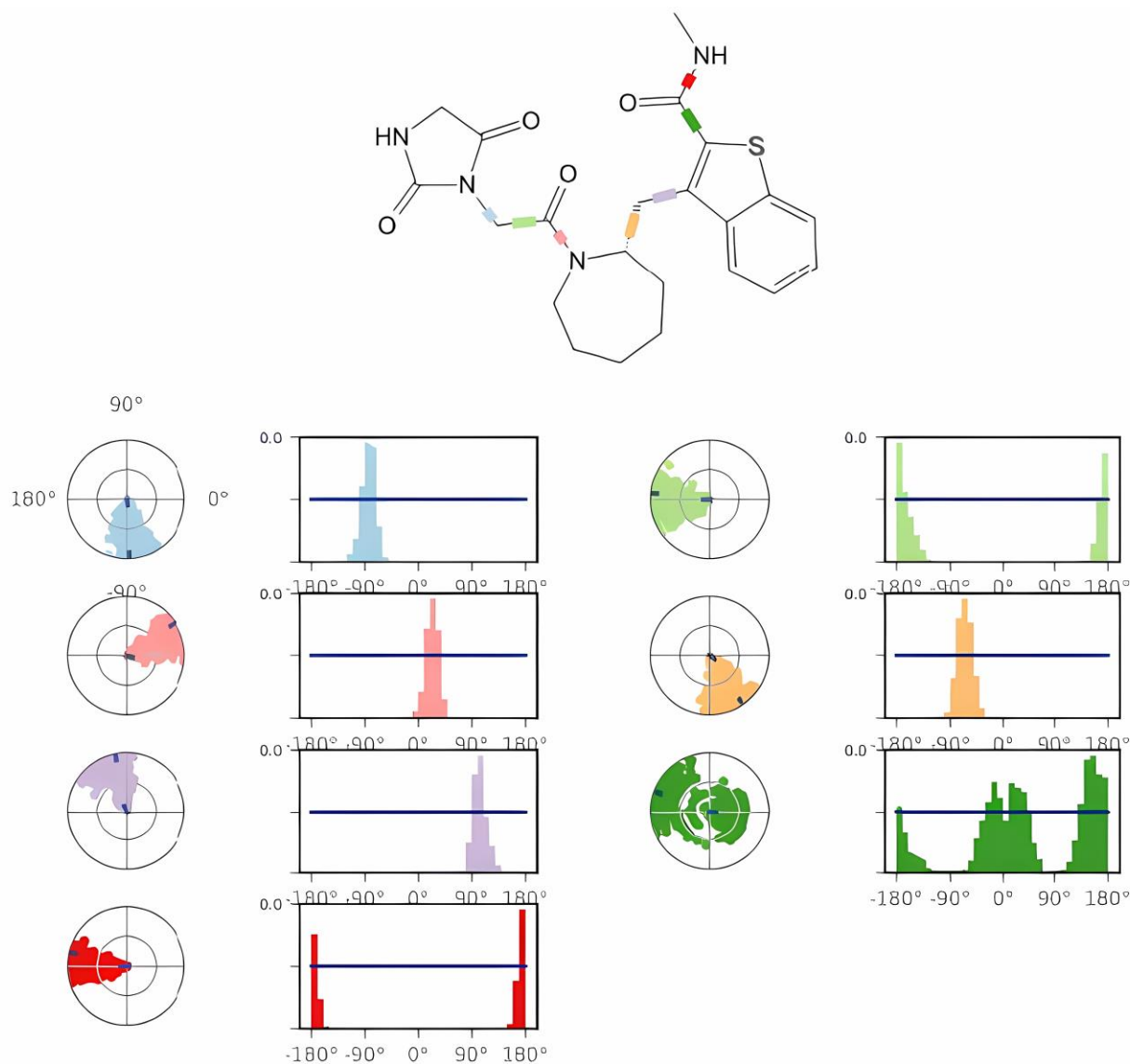


Figure 11: Ligand Torsion Profile of **018**.

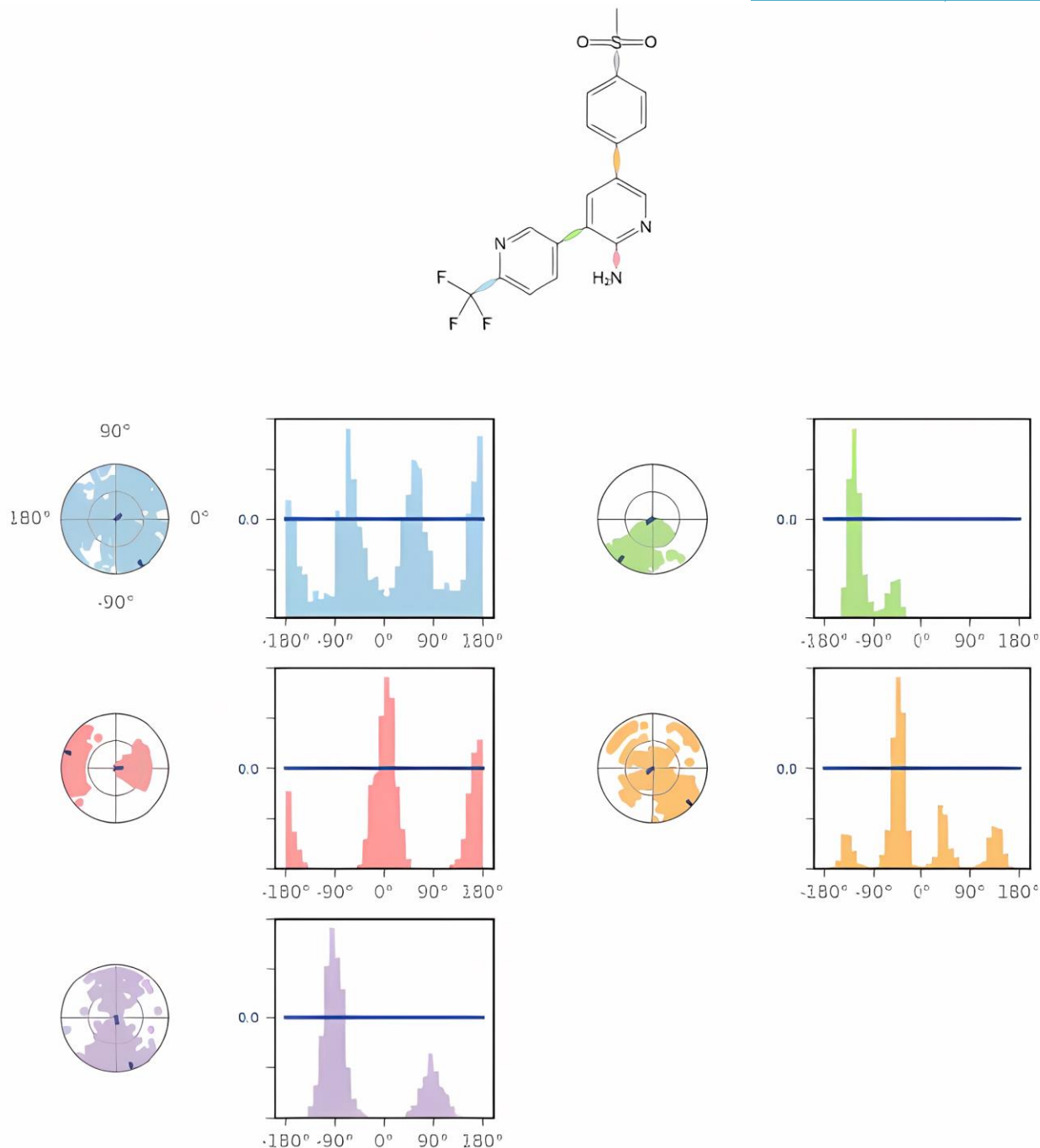


Figure 12: Ligand Torsion Profile of MMV048.

Root Mean Square Fluctuation (RMSF)

The RMSF graphs of **018** and **MMV048** are shown in **Figures 13** and **14**, respectively. The RMSF graphs characterize local changes along the protein chain. The protein residues interacting with the ligand are marked with green-colored vertical bars.

We can observe that the average RMSF of ligand **018** is lower and has less fluctuations than the RMSF of ligand **MMV048**.

This renders ligand **018** more stable in the active site than **MMV048**.

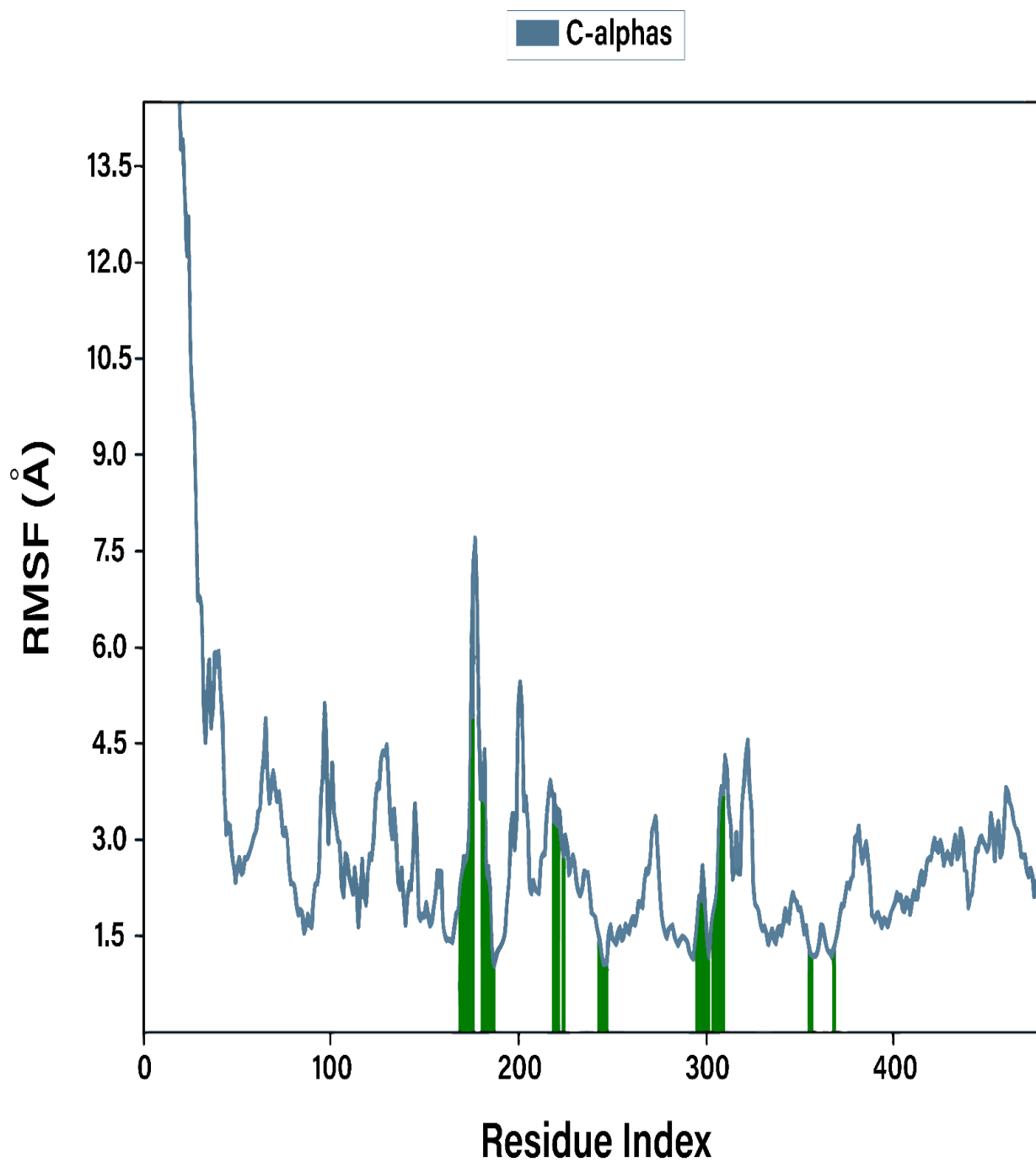


Figure 13: Root Mean Square Fluctuation (RMSF) of **018**.

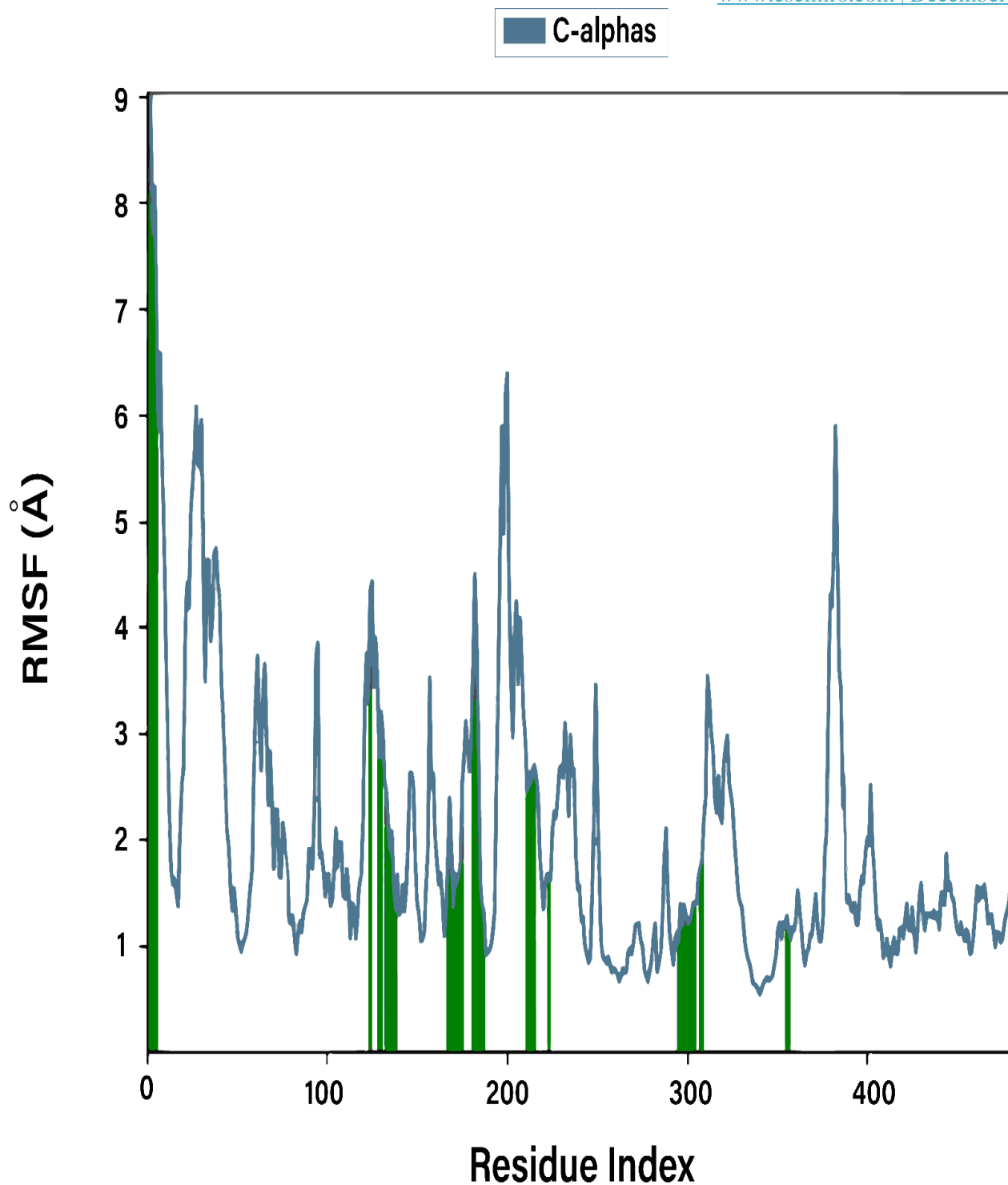


Figure 14: Root Mean Square Fluctuation (RMSF) of MMV048.

Molecular mechanics with generalised Born and surface area solvation (MM/GBSA)**Table 2:** MM/GBSA energy table of the analyzed complexes. ΔG depicts energy change by subtraction of total energy of the receptor and ligand from the complex. All values are in kcal/mol.

Compound	MMGBSA_dG_ Bind	MMGBSA_dG_ _Bind_Solv_GB	MMGBSA_dG_Bind_ VDW	MMGBSA Efficiency	Ligand
018(HIT)	-49.4720	25.1432	-47.3200	-1.5959	
MMV048	-30.0314	1.2528	-23.4456	-1.1123	

From these results, it can be observed that the hit ligand showed more negative scores than the renowned ligand. A more negative value is desirable as it means better stability. Ligand **018** also shows a higher solvation score of 25.1432, which suggests that it has a high binding affinity. Solvation has an effect on the physicochemical properties of a drug. Drugs that are highly solvated have better binding properties.[22] MMV048 has a lower solvation score of 1.2528 hence a lower binder affinity

Methods and Materials

The homology model used in this study was previously described by Ncube et al. [9] The structure-based virtual screening (VS) workflow on Schrödinger Suites was the one followed for this study. The first step involved inputting and generating unique properties for each input compound. The next step is filtering using Lipinski's rule of five for drug-likeness. Lipinski's rules were developed in 1997 by Christopher Lipinski from Pfizer and were among the first to be used to define drug likeness [23]. Also, ligands with reactive functional groups were removed. Preparing the ligands for screening using the Lig-prep function. Ligand preparation allows for the generation of conformers and tautomers to account for many ligand orientations to be generated to find the best binding pose. Lig-prep also allows for removing unstable conformers that may not be docked successfully. After Lig-prep, the receptor is inputted, and the receptor grid generated from docking is the same one that was used for virtual screening. These settings were then written to a file, as VS cannot be run locally. The setup files were then transferred to the Center of High Performance (CHPC) cluster and VS was then carried out on a supercomputer provided by the CHPC.

Set A and Set B were then subjected to Molecular mechanics with generalised Born and surface area solvation (MM/GBSA), and the results were compared. MM/GBSA is a common technique exploited in computational chemistry to calculate the free energy of the binding of ligands to proteins. It is performed after MD as an adjunct to optimizing ligand-receptor complexes [23]. MM/GBSA is done from the frame on the RMSD, where system stability commences. It is run on the part of the simulation where there is convergence. Hence, it must be run from a specific frame until the end to get the average binding energy on the MD trajectory. MM/GBSA can make better predictions than docking scores [24]. Docking scores are not sufficient to establish ligand stability. Their main limitation resides in the estimation of the ligand-receptor interaction. This is often evaluated through simple scoring functions [26]. MM/GBSA calculations on the other hand are mainly performed on an set of protein-ligand

binding conformations which a short MD simulation has generated. These can either be in implicit or explicit solvent. The energy values are calculated using end-point estimates.

The MM/GBSA for the two systems (**018** and **MMV048**) were prepared on Schrödinger Suites. The complexes were loaded on Schrödinger after 100 ns of simulation, and the VSGB solvation model and OPLS4 force field were selected. The files were written and run on a CPU node provided by the CHPC.

Conclusion

The findings of this study showed that structure-based virtual screening is useful in finding novel inhibitors against the *PfPI4KIIIβ* kinase enzyme. The high-throughput virtual screen of various commercial libraries led to the discovery of the three most promising hit compounds, namely **018**, **007** and **009**. Hit compound **018** showed the best RMSD and MM/GBSA results when compared to known ligands of this enzyme, proving that virtual screening (VS) of known and commercial libraries of compounds is an efficient strategy in drug discovery.

In this study, libraries of compounds were combined and docked simultaneously by following the VS workflow. The results from the VS were further confirmed by the MM/GBSA calculations, which showed that those ligands with better docking scores also possessed better binding energies. Binding energy is a critical factor in determining the efficiency of the docking process. This is a successful technique in pursuit of new drug candidates. The hit compounds discovered in this work can either be synthesized or purchased and *in vitro* lab assays can be done to validate the findings from the computational calculations. VS thus saves manufacturers time as filtering ligands through VS narrows down the pool, and only promising ligands can be prioritized for synthesis, thus saving production costs and time.

Declarations

Ethical Approval

Not applicable

Funding

Not applicable

References

1. Walker NF, Nadjm B, Whitty CJM (2014) *Malaria Med* (United Kingdom) 42: 100-106.
2. CDC Mosquito Lifecycle | Dengue | CDC Centres Dis Control Prev 2016.
3. Mita T, Tachibana SI, Hashimoto M, Hirai M (2016) *Plasmodium Falciparum* Kelch 13: A Potential Molecular Marker for Tackling Artemisinin-Resistant Malaria Parasites. *Expert Rev Anti Infect Ther* 14(1): 125-135.
4. Rajkhowa S, Borah SM, Jha AN, Deka RC (2017) Design of *Plasmodium falciparum* PI(4)KIIIβ Inhibitor using Molecular Dynamics and Molecular Docking Methods. *Chemistry Select* 2(5): 1783-1792.

5. Kumar S, Bhardwaj TR, Prasad DN, Singh RK (2018) Drug Targets For Resistant Malaria: Historic To Future Perspectives. *Biomed Pharmacother* 104: 8-27.
6. Tabuti JRS (2008) Herbal Medicines Used in the Treatment of Malaria in Budiope County. *Uganda J Ethnopharmacol* 116(1): 33-42. doi:10.1016/j.jep.2007.10.036.
7. Kibret S, Glenn Wilson G, Ryder D, Tekie H, Petros B (2018) Can Water-Level Management Reduce Malaria Mosquito Abundance Around Large Dams In Sub-Saharan Africa? *PLoS One* 13(4): e0196064
8. Pryce J, Choi L, Richardson M, Malone D (2018) Insecticide Space Spraying for Preventing Malaria Transmission. *Cochrane Database Syst Rev* 11(11): CD012689.
9. Hyde JE (2007) Drug-Resistant Malaria - An Insight. *FEBS J* 274(18): 4688-4698.
10. Mcnamara CW, Lee MCS, Lim CS, Lim SH, Roland J, et al. (2014) Targeting Plasmodium Phosphatidylinositol 4-Kinase To Eliminate Malaria. *Nature* 504(7479): 248-253.
11. Arendse LB, Wyllie S, Chibale K, Gilbert IH (2021) Plasmodium Kinases as Potential Drug Targets for Malaria: Challenges and Opportunities. *ACS Infect Dis* 7(3): 518-534.
12. Ibrahim MAA, Abdelrahman AHM, Hassan AMA (2019) Identification of Novel *Plasmodium Falciparum* PI4KB Inhibitors as Potential Antimalarial Drugs: Homology Modeling, Molecular Docking And Molecular Dynamics Simulations. *Comput Biol Chem* 80: 79-89.
13. Street LJ, Wirjanata G, de Kock C, Wittlin S, Fidock DA, et al. (2018) UCT943, A Next-Generation *Plasmodium falciparum* PI4K Inhibitor Preclinical Candidate for the Treatment of Malaria . *Antimicrob Agents Chemother* 62(9): e00012-e0001218.
14. Ncube NB, Govender KK, Tukulula MA (2023) Critical Analysis of the Binding Pocket of *Plasmodium Falciparum* Phosphatidylinositol-4-Kinase Enzyme. *ChemistrySelect* 8: e202302189.
15. da Silva AM, Ribeiro RIMA, Costa MS, Maia EHB Lima IG, et al (2017) Octopus: A Platform For The Virtual High-Throughput Screening of A Pool of Compounds Against A Set of Molecular Targets. *J Mol Model* 23:26
16. Greenfield DA, Schmidt HR, Skiba MA, Mandler MD, Anderson JR, et al. (2020) Virtual Screening for Ligand Discovery at the σ 1 Receptor. *ACS Med. Chem. Lett.* 11(8): 1555-1561.
17. Vilar S, Ferino G, Phatak SS, Berk B, Civasotto CN, et al. (2011) Docking-Based Virtual Screening For Ligands of G Protein-Coupled Receptors: Not Only Crystal Structures But Also in Silico Models. *J Mol Graph Model* 29(5): 614-623
18. Carugo O, Pongor SA (2001) Normalized Root-Mean-Square Distance for Comparing Protein Three-Dimensional Structures. *Protein Sci* 10(7): 1470-1473.

19. Godschalk F, Genheden S, Söderhjelm P, Ryde U (2013) Comparison of MM/GBSA Calculations Based on Explicit and Implicit Solvent Simulations. *Phys Chem Chem Phys* 15: 7731-7739.
20. Albantova AMA, Goloshchapov AN, Matienko LI, Mil EM, Albantova AA, (2023) The Role H-Bonding and Supramolecular Structures in Homogeneous and Enzymatic Catalysis. *Int J Mol Sci* 24(23): 16874.
21. Schrödinger: Molecular and Materials Simulation Software | Department of Chemistry Available online: <https://chemistry.uconn.edu/2016/07/22/Schrödinger-molecular-and-materials-simulation-software>.
22. Yoshida N (2017) Role of Solvation in Drug Design as Revealed by the Statistical Mechanics Integral Equation Theory of Liquids. *J Chem Inf Model* 57: 2646-2656.
23. Genheden S, Ryde U (2015) The MM/PBSA and MM/GBSA Methods to Estimate Ligand-Binding Affinities. *Expert Opin Drug Discov* 10(5): 449-461. doi:10.1517/17460441.2015.1032936.
24. Hou T, Wang J, Li Y, Wang W (2011) Assessing the Performance of the Molecular Mechanics/Poisson Boltzmann Surface Area and Molecular Mechanics/Generalized Born Surface Area Methods. II. the Accuracy of Ranking Poses Generated From Docking. *J Comput Chem* 32(5): 866-77. doi:10.1002/jcc.21666.
25. Zhang X, Perez-Sanchez H, Lightstone FC (2017) A Comprehensive Docking and MM/GBSA Rescoring Study of Ligand Recognition upon Binding Antithrombin. *Curr Top Med Chem* 17(14): 1631-1639.

Supplementary Table S1

Table S1: Hit Structures from XP virtual screening

Entry Name	Title	Docking score(kcal/mol)
Maybridge_GPCR_Library.2458	LIGPREP-007	-9.065
Maybridge_GPCR_Library.5029	LIGPREP-018	-8.809
Maybridge_Kinase_Library.883	LIGPREP-009	-8.540
Maybridge_GPCR_Library.12167	LIGPREP-016	-8.484
Maybridge_HitCreator_V2.1030	LIGPREP-019	-8.289
Maybridge_Kinase_Library.9920	LIGPREP-019	-7.933
Maybridge_PPI_Library.6728	LIGPREP-011	-7.865
Maybridge_GPCR_Library.4916	LIGPREP-005	-7.793
Maybridge_HitCreator_V2.4143	LIGPREP-012	-7.770
Maybridge_GPCR_Library.3236	LIGPREP-005	-7.727
Maybridge_GPCR_Library.3147	LIGPREP-016	-7.722
Maybridge_Screening_Fragments.57514	LIGPREP-005	-7.703
Maybridge_HitDiscover.26997	LIGPREP-006	-7.703
Maybridge_PPI_Library.6742	LIGPREP-005	-7.651
Maybridge_GPCR_Library.7184	LIGPREP-013	-7.595
Maybridge_HitCreator_V2.636	LIGPREP-005	-7.573
Maybridge_GPCR_Library.3376	LIGPREP-005	-7.571
Maybridge_GPCR_Library.2479	LIGPREP-008	-7.518
Maybridge_PPI_Library.4033	LIGPREP-016	-7.496
Maybridge_Screening_Fragments.31543	LIGPREP-014	-7.409
Maybridge_GPCR_Library.9887	LIGPREP-016	-7.339
Maybridge_HitDiscover.1096	LIGPREP-005	-7.321
Maybridge_Screening_Fragments.16286	LIGPREP-017	-7.319
Maybridge_Screening_Collection.13024	LIGPREP-016	-7.310
Maybridge_Kinase_Library.4346	LIGPREP-012	-7.307
Maybridge_PPI_Library.6924	LIGPREP-007	-7.290
Maybridge_Kinase_Library.971	LIGPREP-017	-7.290
Maybridge_HDAC_Library.2944	LIGPREP-006	-7.284
Maybridge_GPCR_Library.5053	LIGPREP-002	-7.276
Maybridge_PPI_Library.6689	LIGPREP-012	-7.269
Maybridge_GPCR_Library.2662	LIGPREP-011	-7.236
Maybridge_PPI_Library.5050	LIGPREP-013	-7.214
Maybridge_HDAC_Library.1487	LIGPREP-009	-7.207
Maybridge_Screening_Collection.8119	LIGPREP-011	-7.206
Maybridge_HitDiscover.2111	LIGPREP-020	-7.206
Maybridge_GPCR_Library.2509	LIGPREP-018	-7.198

Maybridge_GPCR_Library.2706	LIGPREP-015	-7.142
Maybridge_PPI_Library.5774	LIGPREP-017	-7.137
Maybridge_Screening_Fragments.11155	LIGPREP-006	-7.132
Maybridge_Screening_Collection.12255	LIGPREP-007	-7.122
Maybridge_GPCR_Library.2616	LIGPREP-005	-7.117
Maybridge_HDAC_Library.3538	LIGPREP-020	-7.117
Maybridge_PPI_Library.3075	LIGPREP-018	-7.084
Maybridge_GPCR_Library.4872	LIGPREP-001	-7.014
Maybridge_Kinase_Library.10258	LIGPREP-013	-7.010
Maybridge_PPI_Library.2619	LIGPREP-002	-6.998
Maybridge_PPI_Library.900	LIGPREP-003	-6.988
Maybridge_Kinase_Library.6902	LIGPREP-008	-6.988
Maybridge_GPCR_Library.7039	LIGPREP-008	-6.983
Maybridge_Screening_Fragments.36174	LIGPREP-005	-6.981
Maybridge_HitDiscover.32868	LIGPREP-017	-6.973
Maybridge_Screening_Fragments.8423	LIGPREP-014	-6.963
Maybridge_Screening_Collection.52458	LIGPREP-010	-6.959
Maybridge_Screening_Collection.6778	LIGPREP-010	-6.956
Maybridge_GPCR_Library.5070	LIGPREP-019	-6.951
Maybridge_Kinase_Library.10541	LIGPREP-011	-6.938
Maybridge_HitCreator_V2.4020	LIGPREP-009	-6.921
Maybridge_HitDiscover.29709	LIGPREP-018	-6.916
Maybridge_Screening_Fragments.15479	LIGPREP-010	-6.868
Maybridge_GPCR_Library.5054	LIGPREP-003	-6.851
Maybridge_HitDiscover.46776	LIGPREP-005	-6.843
Maybridge_Screening_Collection.33997	LIGPREP-009	-6.843
Maybridge_Screening_Fragments.38147	LIGPREP-018	-6.834
Maybridge_GPCR_Library.7200	LIGPREP-009	-6.826
Maybridge_HitCreator_V2.9158	LIGPREP-007	-6.825
Maybridge_Screening_Collection.13025	LIGPREP-017	-6.817
Maybridge_Screening_Fragments.16287	LIGPREP-018	-6.817
Maybridge_Kinase_Library.968	LIGPREP-014	-6.814
Maybridge_HDAC_Library.28	LIGPREP-010	-6.799
Maybridge_PPI_Library.1876	LIGPREP-019	-6.794
Maybridge_GPCR_Library.2112	LIGPREP-001	-6.772
Maybridge_GPCR_Library.4884	LIGPREP-013	-6.764
Maybridge_Kinase_Library.6431	LIGPREP-017	-6.760
Maybridge_GPCR_Library.7196	LIGPREP-005	-6.759
Maybridge_GPCR_Library.4089	LIGPREP-018	-6.759
Maybridge_PPI_Library.5035	LIGPREP-018	-6.755
Maybridge_HitCreator_V2.8929	LIGPREP-018	-6.740

Maybridge_Screening_Fragments.43604	LIGPREP-015	-6.733
Maybridge_GPCR_Library.2622	LIGPREP-011	-6.717
Maybridge_GPCR_Library.13895	LIGPREP-004	-6.714
Maybridge_PPI_Library.2436	LIGPREP-019	-6.714
Maybridge_HDAC_Library.3594	LIGPREP-016	-6.712
Maybridge_PPI_Library.1783	LIGPREP-006	-6.704
Maybridge_GPCR_Library.2613	LIGPREP-002	-6.692
Maybridge_GPCR_Library.13329	LIGPREP-018	-6.689
Maybridge_GPCR_Library.4997	LIGPREP-006	-6.687
Maybridge_HitCreator_V2.626	LIGPREP-015	-6.686
Maybridge_GPCR_Library.2460	LIGPREP-009	-6.683
Maybridge_PPI_Library.7170	LIGPREP-013	-6.676
Maybridge_PPI_Library.3368	LIGPREP-011	-6.673
Maybridge_PPI_Library.6772	LIGPREP-015	-6.673
Maybridge_HDAC_Library.1173	LIGPREP-015	-6.671
Maybridge_Screening_Collection.32095	LIGPREP-007	-6.671
Maybridge_GPCR_Library.8577	LIGPREP-006	-6.670
Maybridge_GPCR_Library.4892	LIGPREP-001	-6.669
Maybridge_HitCreator_V2.842	LIGPREP-011	-6.662
Maybridge_GPCR_Library.7688	LIGPREP-017	-6.659
Maybridge_GPCR_Library.7056	LIGPREP-005	-6.658
Maybridge_GPCR_Library.11995	LIGPREP-004	-6.645
Maybridge_GPCR_Library.7606	LIGPREP-015	-6.636
Maybridge_HitCreator_V2.1940	LIGPREP-009	-6.632
Maybridge_Kinase_Library.9513	LIGPREP-018	-6.631
Maybridge_HitDiscover.24650	LIGPREP-019	-6.628
Maybridge_Kinase_Library.3578	LIGPREP-004	-6.626
Maybridge_Screening_Collection.22898	LIGPREP-010	-6.623
Maybridge_Kinase_Library.3397	LIGPREP-003	-6.622
Maybridge_PPI_Library.6970	LIGPREP-013	-6.620
Maybridge_HitDiscover.48295	LIGPREP-004	-6.617
Maybridge_PPI_Library.6746	LIGPREP-009	-6.612
Maybridge_PPI_Library.7003	LIGPREP-006	-6.611
Maybridge_GPCR_Library.2555	LIGPREP-004	-6.604
Maybridge_Kinase_Library.659	LIGPREP-005	-6.602
Maybridge_GPCR_Library.11361	LIGPREP-010	-6.601
Maybridge_PPI_Library.295	LIGPREP-018	-6.601
Maybridge_GPCR_Library.5066	LIGPREP-015	-6.600
Maybridge_GPCR_Library.7205	LIGPREP-014	-6.595
Maybridge_PPI_Library.2834	LIGPREP-017	-6.593
Maybridge_PPI_Library.6914	LIGPREP-017	-6.582

Maybridge_Screening_Fragments.37167	LIGPREP-018	-6.582
Maybridge_GPCR_Library.7208	LIGPREP-017	-6.580
Maybridge_Kinase_Library.7260	LIGPREP-006	-6.578
Maybridge_PPI_Library.6963	LIGPREP-006	-6.573
Maybridge_HitDiscover.35230	LIGPREP-019	-6.570
Maybridge_Screening_Collection.43112	LIGPREP-004	-6.567
Maybridge_Screening_Fragments.47613	LIGPREP-004	-6.567
Maybridge_PPI_Library.1874	LIGPREP-017	-6.564
Maybridge_Screening_Collection.33033	LIGPREP-005	-6.563
Maybridge_HitDiscover.39707	LIGPREP-016	-6.552
Maybridge_HitDiscover.45635	LIGPREP-004	-6.549
Maybridge_GPCR_Library.2908	LIGPREP-017	-6.548
Maybridge_PPI_Library.7029	LIGPREP-012	-6.546
Maybridge_PPI_Library.3073	LIGPREP-016	-6.544
Maybridge_HitCreator_V2.4696	LIGPREP-005	-6.535
Maybridge_GPCR_Library.13698	LIGPREP-007	-6.529
Maybridge_GPCR_Library.7179	LIGPREP-008	-6.528
Maybridge_GPCR_Library.4257	LIGPREP-006	-6.528
Maybridge_PPI_Library.17	LIGPREP-020	-6.527
Maybridge_Screening_Collection.18884	LIGPREP-016	-6.527
Maybridge_HDAC_Library.401	LIGPREP-003	-6.521
Maybridge_HitCreator_V2.8804	LIGPREP-013	-6.517
Maybridge_Kinase_Library.7631	LIGPREP-017	-6.516
Maybridge_Screening_Collection.51109	LIGPREP-001	-6.511
Maybridge_Screening_Fragments.56131	LIGPREP-002	-6.511
Maybridge_HitDiscover.20554	LIGPREP-003	-6.511
Maybridge_GPCR_Library.1671	LIGPREP-020	-6.507
Maybridge_Kinase_Library.6951	LIGPREP-017	-6.503
Maybridge_GPCR_Library.12737	LIGPREP-006	-6.499
Maybridge_GPCR_Library.2772	LIGPREP-001	-6.497
Maybridge_Kinase_Library.4116	LIGPREP-002	-6.496
Maybridge_Kinase_Library.7627	LIGPREP-013	-6.494
Maybridge_Screening_Fragments.26228	LIGPREP-019	-6.490
Maybridge_Screening_Collection.52592	LIGPREP-004	-6.485
Maybridge_PPI_Library.5538	LIGPREP-001	-6.485
Maybridge_Screening_Collection.21399	LIGPREP-011	-6.477
Maybridge_GPCR_Library.4993	LIGPREP-002	-6.474
Maybridge_GPCR_Library.8189	LIGPREP-018	-6.471
Maybridge_Kinase_Library.339	LIGPREP-005	-6.458
Maybridge_GPCR_Library.2455	LIGPREP-004	-6.455
Maybridge_IonChannel_Library.4962	LIGPREP-006	-6.454

Maybridge_Screening_Fragments.24727	LIGPREP-018	-6.454
Maybridge_HitDiscover.15973	LIGPREP-002	-6.449
Maybridge_HitCreator_V2.2287	LIGPREP-016	-6.447
Maybridge_PPI_Library.1287	LIGPREP-010	-6.441
Maybridge_GPCR_Library.7310	LIGPREP-019	-6.441
Maybridge_GPCR_Library.7771	LIGPREP-020	-6.441
Maybridge_Kinase_Library.6977	LIGPREP-003	-6.440
Maybridge_Screening_Fragments.43674	LIGPREP-005	-6.436
Maybridge_Screening_Collection.39256	LIGPREP-008	-6.436
Maybridge_GPCR_Library.5860	LIGPREP-009	-6.433
Maybridge_Screening_Collection.52356	LIGPREP-008	-6.432
Maybridge_GPCR_Library.12370	LIGPREP-019	-6.424
Maybridge_Screening_Fragments.43640	LIGPREP-011	-6.422
Excel.1690	LIGPREP-002	-6.421
Maybridge_Screening_Collection.22294	LIGPREP-006	-6.420